Further investigations of the low-lying electronic states of AsO^+ radical*

Zhu Zun-Lue(朱遵略)†, Qiao Hao(乔 浩), Lang Jian-Hua(郎建华), and Sun Jin-Feng(孙金锋)

College of Physics and Electronic Engineering, Henan Normal University, Xinxiang 453007, *China*

(Received 10 April 2013; revised manuscript received 18 May 2013)

The high level quantum chemistry *ab inito* multi-reference configuration interaction (MRCI) method with large V5Z basis set is used to calculate the spectroscopic properties of the 15 Λ–S electronic states ($X^1\Sigma^+$, $A^1\Pi$, $^1\Delta$, $^1\Sigma^-$, $^3\Sigma^+$, $^3\Pi$, $^3\Delta$, $^3\Sigma^-$, $^5\Sigma^+$, $^5\Pi$, $^5\Delta$, $^1\Pi$ (II), $^5\Sigma^+$ (II), $^1\Pi$ (III), and $^1\Pi$ (IV)) of AsO^+ radical correlated to the dissociation limit $As^+(^3P_g)$ + $O(^3P_g)$ and $As^+(^1D_g)$ + $O(^1D_g)$. In order to obtain better potential curves and more accurate spectroscopic properties, the Davidson modification is taken into account. With the potential energy curves (PECs) determined here, vibrational levels $G(\upsilon)$ and inertial rotation constants B_υ are computed for all the bound electronic states when the rotational quantum number J equals zero ($J = 0$). Except for the states $X^1\Sigma^+$, $A^1\Pi$, it is the first time that the multi-reference configuration calculation has been used on the 13 Λ–S electronic states of the AsO^+ radical. The potential energy curves of all the Λ–S electronic states are depicted according to the avoided crossing rule of the same symmetry. Spin–orbit coupling effect (SOC) is introduced into the states $X^1\Sigma^+$, $A^1\Pi$, $^3\Pi$ to consider its effects on the spectroscopic properties. Transition dipole moments (TDMs) from $A^1\Pi_1$, $^3\Pi_1$ states to the ground state $X^1\Sigma^+_{0+}$ are predicted as well.

Keywords: MRCI (+Q), spin–orbit coupling effect (SOC), potential energy curves (PECs), spectroscopic constants

PACS: 31.50.–x, 34.20.–b, 31.15.A–, 33.15.Mt **DOI:** 10.1088/1674-1056/22/10/103102

1. Introduction

China is the largest producer of white arsenic, accounting for fifty percent of world reserves, and arsenic oxide are widely used in medicine and agriculture. Nowadays, arsenic oxide has been playing an increasingly important role in medicine and agriculture. So the study on arsenic and its oxides are rather significant at present.

With the development of the calculation methods of the quantum chemistry, *ab initio* calculations can give more and more accurate potential energy curves (PECs) for diatomic molecules. Moreover, according to the PECs, one can determine the spectroscopic constants by solving the Schrödinger equation of nuclear motion. Therefore, it is an effective way to investigate the spectroscopic properties of diatomic molecules.[1–6] As the hetero-nuclear radical involves the As cation and O atom, the electronic structure of the AsO^+ radical has been investigated not only experimentally, but also theoretically in the past several decades. Early theoretical results on the spectroscopic constants of the ground state $X^1\Sigma^+$ and one low-lying excited state $A^1\Pi$ of AsO^+ radical were summarized by Lakshman and Rao[7] in 1970. In 2012, *ab initio* calculation was carried out by Wang *et al.*[8] at the theoretical level of As/aug-cc-pV5Z and O/aug-cc-pV6Z to determine spectroscopic constants of the AsO^+ radical. Experimentally, the studies concentrated on the spectral properties of the AsO^+ radical in the nineteenth century.[9–15] Lakshman and Rao[9] reported on the band spectrum on the AsO^+ radical inthe UV region of wavelength in a range of 2200 Å·nm–2250 Å·nm in 1960. Two years later, Santaram and Rao[10] continued to investigate this system in detail, and gave the rotational constants of the ground state $X^1\Sigma^+$ and low excited state $A^1\Pi$. However, Rao and some people made much closer study on this area under conditions of high resolution in 1970,[11] they confirmed that the transition is $^1\Pi - ^1\Sigma^+$, not $^1\Sigma^+ - ^1\Sigma^+$ by analyzing the 4–0, 3–0, 2–0, 1–0, and 1–1 spectral bands. In 1966, Lakshman[12] studied the spectra in some ranges where the wavelength is near 2100 Å and obtained the new band from the $A^1\Pi - ^1\Sigma^+$ system. Shanker *et al.*[13] recorded (1, 0) and (2, 0) spectral bands of the $A^1\Pi - ^1\Sigma^+$ system in 1969. In the same year, Rao D V K and Rao P T[14] studied (1, 0) and (2, 0) spectral bands of the $A^1\Pi$–$^1\Sigma^+$ system again, and gave the spectroscopic constants and molecular constants of two states. The spectroscopic constants and molecular constants on the AsO^+ radical in the early years were kept in the books which were published in 1979, such as Huber and Herzberg.[15]

At the present time, the MRCI + Q[16,17] method is still the most stable and reliable method for high accuracy calculation of the electronic state structure, especially for large bond length problems. In the present work, the 15 low-lying electronic states of the AsO^+ radical are calculated based on the MRCI + Q[16,17] method, in which the states $X^1\Sigma^+$, $A^1\Pi$, $^1\Delta$, $^1\Sigma^-$, $^3\Sigma^+$, $^3\Pi$, $^3\Delta$, $^3\Sigma^-$, $^5\Sigma^+$, $^5\Pi$, $^1\Pi$ (III) are bound electronic

*Project supported by the National Natural Science Foundation of China (Grant Nos. 11274097 and 61275132) and the Natural Science Foundation of Henan Province, China (Grant No. 2008A140008).

†Corresponding author. E-mail: zl-zhu@htu.cn

© 2013 Chinese Physical Society and IOP Publishing Ltd

states. The spectroscopic properties, vibrational levels $G(\upsilon)$, and inertial rotation constants B_υ of all the bound electronic states are obtained. Meanwhile, the spin–orbit coupling effect is introduced into the states $X^1\Sigma^+$, $A^1\Pi$, $^3\Pi$ to split into 6Ω states. And the transition dipole moments (TDMs) from $A^1\Pi_1$, $^3\Pi_1$ states to the ground state $X^1\Sigma^+_{0+}$ are predicted as well. In the calculation, all the PECs and spectroscopic constants are fitted with considering the avoided crossing rule between states of the same symmetry.

2. Computational detail

The calculation is launched with the aid of the *ab initio* quantum chemistry program package MOLPRO 2008.1.[18] Here, the PECs of electronic states including 15 Λ–S electronic states and 6Ω electronic states for the AsO^+ radical are calculated. Based on the calculated PECs, the spectroscopic parameters (R_e, T_e, ω_e, $\omega_e x_e$, B_e, D_e), vibrational levels $G(\upsilon)$, and inertial rotation constants B_υ are determined by solving the nuclear Schrödinger equation with the aid of module VIBROT in the MOLCAS 7.4 program package.[19]

In order to guarantee the accuracy of the PECs, all the calculations are made with the full valence complete active space self-consistent field (CASSCF) method[20] followed by the highly accurate valence internally contracted MRCI approach.[21,22] The all-electron basis sets cc-pV5Z is selected for As^+ cation and O atom in computation. Based on the above method, the bond length is calculated in steps of 0.005 nm to scan a series of the single-point energies over a nuclear separation range from 0.1 nm to 0.6 nm. In computation, firstly, the restricted Hartree–Fock (RHF) method is adopted to generate the ground-state wave function; then, the obtained wave function is optimized by using the state-averaged complete active space self-consistent-field method,[23,24] where the weight factors of the configuration are improved. Finally, the internally contracted multi-reference configuration interaction (MRCI) approach is employed to perform the correlation energy calculation to obtain the accurate energies based on the acquired optimized reference wave function in the state-averaged complete active space self-consistent-field calculation. The PECs of these 15 Λ–S electronic states are drawn with continuous energy points with the aid of the avoided crossing rule of the same symmetry. Because the energies from the MRCI calculation are not equipped with the size extensivity, which is of great significance for the dissociation of potential energy curve, therefore, the Davidson modification (+Q) is taken into account in the present calculation to correct the size extensivity error.

Because of the limitation of the MOLPRO program package, all the calculations are carried out in C_{2v} symmetry with the order of the irreducible representations $a_1/b_1/b_2/a_2$. In the calculation, eight molecular orbitals (MOs) are put into active space, including four a_1, two b_1, two b_2 symmetry MOs, which correspond to the 2s2p shells of the O atom and 4s4p shells of the As^+ cation. The rest of the electrons are put into the closed-shell orbits (eight a_1, three b_1, three b_2, and one a_2). Namely, there are totally ten electrons of the AsO^+ radical being used in the electronic correlation energy calculation. But, all these PECs are not smooth by employing these MOs (twelve a_1, five b_1, five b_2, and one a_2). Analysis shows that this situation is caused by skipping from the PEC of one state to another. To improve the smoothness of these PECs, one additional a_1 MO is put into the active space, in other words, nine MOs are put into active space (five a_1, two b_1, and two b_2). Using these MOs (thirteen a_1, five b_1, five b_2, and one a_2), the PECs of these fifteen electronic states calculated at the present level of theory are smooth and convergent over the present internuclear separation range.

The spin–orbit coupling effect (SOC) is introduced into the present work. In the SOC calculation, the state interaction method is employed, which means that the matrixes of $H_{el} + H_{SO}$ based on the basis of eigenfunctions of H_{el} are diagonalized to acquire the spin–orbit coupling eigenstates. In this process, the H_{el} and H_{SO} come from the state-averaged complete active space self-consistent-field and MRCI + Q calculation, respectively. The SOC PECs are plotted with the aid of the avoided crossing rule of the same symmetry.

Based on the PECs of the Λ–S and Ω electronic states, the spectroscopic constants, including the equilibrium internuclear distance R_e, dissociation energy D_e, excitation energy T_e, vibration constants ω_e, and $\omega_e x_e$, balanced rotation constant B_e are determined by numerically solving the one-dimensional nuclear Schrödinger equation. Meanwhile, vibrational level $G(\upsilon)$ and inertial rotation constant B_υ are also computed for all the bound electronic states when $J = 0$.

3. Results and discussion

3.1. Potential energy curves of the 15 Λ–S electronic states

The PECs of the 15 Λ–S electronic states of the AsO^+ radical are calculated at the level of MRCI + Q/V5Z. The achieved PECs are plotted in Fig. 1, where the states $X^1\Sigma^+$, $A^1\Pi$, $^1\Delta$, $^1\Sigma^-$, $^3\Sigma^+$, $^3\Pi$, $^3\Delta$, $^3\Sigma^-$, $^5\Sigma^+$, $^5\Pi$, $^5\Delta$, $^5\Sigma^+$ (II), $^1\Pi$ (II) are correlated with the dissociation limits of the ground states $As^+(^3P_g)$ and $O(^3P_g)$, while the rest of two states $^1\Pi$ (III) and $^1\Pi$ (IV) are correlated with the dissociation limit of the first excited state $As^+(^1D_g)$ and the first excited state $O(^1D_g)$. The dissociation limits and the corresponding energy gap are summarized in Table 1. The calculated energy gap of 25579.42 cm^{-1} between two dissociation limits is in good agreement with the available experimental result of 25963.68 cm^{-1}.[25] Based on the calculated PECs, the spectroscopic constants of the bound electronic states are determined and listed in Table 2, where the main ten-valence-electron configurations at R_e are given as well.

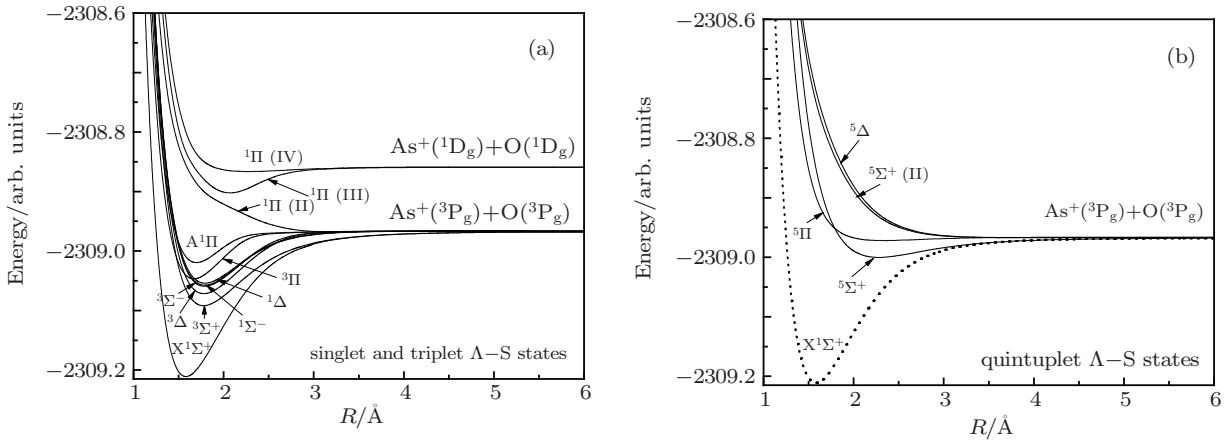


Fig. 1. Potential energy curves of 15 Λ–S electronic states of AsO^+ (a) singlet and triplet Λ–S states (b) quintuplet Λ–S states.

Table 1. The dissociation limit relationships of 15 Λ–S electronic states.

Λ–S states	$As^+ + O$	Energy/cm^{-1}	
$X^1\Sigma^+$, $A^1\Pi$, $^1\Delta$, $^1\Sigma^-$, $^3\Sigma^+$, $^3\Pi$, $^3\Delta$, $^3\Sigma^-$, $^5\Sigma^+$, $^5\Pi$, $^5\Delta$, $^5\Sigma^+$ (II), $^1\Pi$ (II)	$As^+(^3P_g) + O(^3P_g)$	0	0
$^1\Pi$ (III), $^1\Pi$ (IV)	$As^+(^1D_g) + O(^1D_g)$	25579.42	25963.68[a]

[a]Data from Ref. [25].

The ground state $X^1\Sigma^+$ is mainly characterized by the closed shell electronic configuration $7\sigma^2 8\sigma^2 9\sigma^2 3\pi^4 4\pi^0$ with the configuration weight factor of 0.80 around the equilibrium position. It has a deep potential well and the depth of the well is 6.87 eV. The equilibrium bond length R_e (0.15789 nm) is close to the theoretical and experimental results.[7,8,14] Compared with the available result,[7,8,14] the equilibrium internuclear distance R_e is somehow 0.00109 nm larger than the value deduced from the Modified Rees method of Lakshman and Rao. And the difference in harmonic frequency ω_e between this work and experiment is only 4.19 cm^{-1}. Meanwhile, the calculated spectroscopic constants $\omega_e x_e$ and B_e in this work are smaller than the experimental data by 0.05 cm^{-1} and 0.0061 cm^{-1}, respectively.

As one electron is stimulated from 9σ orbital to 4π orbital, two excited electronic states $A^1\Pi$, $^3\Pi$ can be generated according to the electronic spin arrangement. The low-lying electronic state $^3\Pi$ results from the primary electronic configuration $7\sigma^2 8\sigma^2 9\sigma^\alpha 3\pi^4 4\pi^\alpha$, where the two electrons respectively from the 9σ and 4π orbit are spin-parallel. Through MRCI + Q calculation, the energy of 2.1625 eV is needed to dissociate the AsO^+ radical of $^3\Pi$ electronic state into the independent $As^+(^3P_g)$ and $O(^3P_g)$. The energy located at the equilibrium position overtops that of the ground state by 35971.81 cm^{-1}. Spin antiparallel of two electrons from the 9σ orbital and 4π orbital confirms the excited state $A^1\Pi$. Although the electronic state $A^1\Pi$ is a bound state, it holds a shallow potential well with D_e of 1.4040 eV. The excitation energy T_e of the state $A^1\Pi$ at R_e is 42558.88 cm^{-1}. The calculated spectroscopic constants ω_e, $\omega_e x_e$, and B_e are 771.918 cm^{-1}, 7.09630 cm^{-1}, and 0.431968 cm^{-1} respectively, which are all in good agreement with the experimental results 780.80 cm^{-1}, 7.4 cm^{-1}, and 0.4491 cm^{-1}.[14]

In addition, the main electronic configuration $7\sigma^2 8\sigma^2 9\sigma^2 3\pi^3 4\pi^1$ of the excited states $^1\Delta$, $^1\Sigma^-$, $^3\Sigma^+$, $^3\Delta$, $^3\Sigma^-$ can form when an electron is excited from 3π orbital to 4π orbital. For these electronic states, the PECs of the states $^1\Delta$ and $^1\Sigma^-$ are rather adjacent over the whole range of internuclear distance. Therefore, the spectroscopic constants are very close. The values of excitation energy T_e of the states $^1\Delta$, $^1\Sigma^-$ are 34111.19 cm^{-1} and 33667.19 cm^{-1} and the difference in vibration constant ω_e between two states is only 7 m^{-1}, with the well depth of two states being almost the same. Besides $^1\Delta$ and $^1\Sigma^-$ states, the states $^1\Sigma^-$ and $^3\Sigma^-$ have the same scenarios as well. Because the states $^1\Delta$, $^1\Sigma^-$, $^3\Sigma^-$ are so adjacent that it is difficult to distinguish from each other in Fig. 1, but the result that corresponds to the energy arrangement from low to high, that is, $^3\Sigma^-$, $^1\Sigma^-$, $^1\Delta$ can be obtained by the excitation energy T_e in Table 2. Meanwhile, the computed results indicate that the first low-lying excited state should be the state $^3\Sigma^+$. Because it has the second well depth except the ground state $X^1\Sigma^+$ and the excitation energy T_e value is 26138 cm^{-1} at the equilibrium bond length of 1.7746 Å. The well depth is 3.6908 eV, which is deeper than those of the rest of excited states.

Table 2. Spectroscopic constants of the 11 Λ–S electronic states.

Λ–S state	T_e/cm^{-1}	R_e/nm	ω_e/cm^{-1}	$\omega_e x_e$/cm^{-1}	B_e/cm^{-1}	D_e/eV	Dominant electron configuration
$X^1\Sigma^+$							$7\sigma^2 8\sigma^2 9\sigma^2 3\pi^4 4\pi^0$ (79.74)
							$7\sigma^2 8\sigma^2 9\sigma^2 3\pi^{\alpha\beta\alpha} 4\pi^{\beta}$ (5.08)
							$7\sigma^2 8\sigma^2 9\sigma^2 3\pi^{\alpha\beta} 4\pi^{\alpha\beta}$ (2.60)
This work	0	0.15789	1095.51	4.95	0.5138	6.87	
Theory[a]	0	0.1568	1100.7	4.83	0.5199	–	
Theory[b]	0	0.15770	1091.07	5.02	0.5148	–	
Exp.[c]	0	0.1568	1091.32	5.00	0.5199	–	
$^3\Sigma^+$							$7\sigma^2 8\sigma^2 9\sigma^{\alpha} 3\pi^{\alpha\beta\alpha} 4\pi^{\alpha}$ (87.15)
This work	26138.55	0.17746	740.89	3.96	0.4051	3.69	
$^3\Delta$							$7\sigma^2 8\sigma^2 9\sigma^2 3\pi^{\alpha\beta\alpha} 4\pi^{\alpha}$ (88.01)
This work	30538.14	0.17766	733.94	3.10	0.4010	2.93	
$^3\Sigma^-$							$7\sigma^2 8\sigma^2 9\sigma^2 3\pi^{\alpha\beta\alpha} 4\pi^{\alpha}$ (86.79)
This work	33271.70	0.17850	705.63	2.08	0.3912	2.57	
$^1\Sigma^-$							$7\sigma^2 8\sigma^2 9\sigma^2 3\pi^{\alpha\beta\alpha} 4\pi^{\beta}$ (86.44)
This work	33667.19	0.17876	704.93	2.88	0.3946	2.48	
$^1\Delta$							$7\sigma^2 8\sigma^2 9\sigma^2 3\pi^{\alpha\beta\alpha} 4\pi^{\beta}$ (87.93)
This work	34111.19	0.17891	697.98	2.75	0.3933	2.45	
$^3\Pi$							$7\sigma^2 8\sigma^2 9\sigma^{\alpha} 3\pi^4 4\pi^{\alpha}$ (84.60)
							$7\sigma^2 8\sigma^{\alpha} 9\sigma^2 3\pi^{\alpha\beta\beta} 4\pi^{\alpha\alpha}$ (1.32)
							$7\sigma^2 8\sigma^2 9\sigma^{\alpha} 3\pi^{\alpha\beta} 4\pi^{\alpha\beta\alpha}$ (1.31)
This work	35971.81	0.16669	801.13	1.86	0.4405	2.21	
$A^1\Pi$							$7\sigma^2 8\sigma^2 9\sigma^{\alpha} 3\pi^4 4\pi^{\beta}$ (80.80)
							$7\sigma^2 8\sigma^{\alpha} 9\sigma^2 3\pi^4 4\pi^{\beta}$ (3.08)
							$7\sigma^2 8\sigma^2 9\sigma^{\alpha} 3\pi^{\alpha\beta} 4\pi^{\alpha\beta\beta}$ (1.34)
This work	42558.88	0.16875	778.91	7.09	0.4319	1.45	
Theory[a]	42599	0.1687	780.77	7.36	0.4491	–	
Theory[b]	42327.96	0.16982	776.84	6.72	0.4433	–	
Exp.[c]	42594.2	0.1688	780.8	7.4	0.4491	–	
$^5\Sigma^+$							$7\sigma^2 8\sigma^2 9\sigma^2 3\pi^{\alpha\alpha} 4\pi^{\alpha\alpha}$ (90.45)
This work	46473.97	0.22749	325.11	4.07	0.2493	1.15	
$^5\Pi$							$7\sigma^2 8\sigma^2 9\sigma^{\alpha} 3\pi^{\alpha\beta\alpha} 4\pi^{\alpha\alpha}$ (91.23)
This work	52624.97	0.23002	168.36	4.83	0.2408	0.15	
$^1\Pi$ (III)							$7\sigma^2 8\sigma^2 9\sigma^2 3\pi^{\alpha\beta\beta} 4\pi^0$ (60.15)
							$7\sigma^2 8\sigma^2 9\sigma^2 3\pi^{\beta\beta} 4\pi^{\alpha}$ (16.72)
							$7\sigma^2 8\sigma^2 9\sigma^2 3\pi^{\beta} 4\pi^{\alpha\beta}$ (4.43)
							$7\sigma^2 8\sigma^2 9\sigma^2 3\pi^{\alpha\beta} 4\pi^{\beta}$ (2.43)
							$7\sigma^2 8\sigma^2 9\sigma^2 3\pi^{\beta} 4\pi^{\alpha\beta}$ (1.73)
This work	67775.74	0.20719	542.83	6.09	0.3838	1.28	

[a]Data from Ref. [7]; [b]Data from Ref. [8]; [c]Data from Ref. [14].

The calculated quintuplet states are purely repulsive except the electronic states $^5\Sigma^+$, $^5\Pi$. To the best of our knowledge, this is the first time that the quintuplet states for AsO^+ radical have been computed with the *ab initio* calculation method. The values of dissociation energy D_e of the $^5\Sigma^+$ and $^5\Pi$ states are 1.1549 eV and 0.1582 eV, and the energies of the equilibrium positions of $^5\Sigma^+$ and $^5\Pi$ states are close to the dissociation limit. So, both of them are very unstable and would be hard to observe. Especially for the $^5\Pi$ state, the D_e is less than 0.2 eV and it has only 10 vibrational levels, which is because the vibration constant ω_e is small.

All the Λ–S states involved in the above discussion correlate to the dissociation limit $As^+(^3P_g) + O(^3P_g)$. For the other dissociation limit $As^+(^1D_g) + O(^1D_g)$, the two Λ–S states, that is, $^1\Pi$ (III) and $^1\Pi$ (IV), are calculated. As one of the two single states, the bound state $^1\Pi$ (III), the third root of $^1\Pi$ symmetry arises from the electronic configurations $7\sigma^2 8\sigma^2 9\sigma^2 3\pi^{\alpha\beta\beta} 4\pi^0$ (60.15), $7\sigma^2 8\sigma^2 9\sigma^2 3\pi^{\beta\beta} 4\pi^{\alpha}$ (16.72), $7\sigma^2 8\sigma^2 9\sigma^2 3\pi^{\beta} 4\pi^{\alpha\beta}$ (4.43), $7\sigma^2 8\sigma^2 9\sigma^2 3\pi^{\alpha\beta} 4\pi^{\beta}$ (2.43), and $7\sigma^2 8\sigma^2 9\sigma^2 3\pi^{\beta} 4\pi^{\alpha\beta}$ (1.73) at the equilibrium position, which demonstrates that the $^1\Pi$ (III) state is obviously multi-configurational in nature and it is essential to employ the multi-reference configuration interaction in our research. Different from the $^1\Pi$ (III), the fourth $^1\Pi$ electronic state is a completely repulsive state.

3.2. Vibrational manifolds

Information about the vibrational level $G(\upsilon)$ and inertial rotation constant B_υ of the electronic state of AsO^+ radical are relatively rare. Using the PECs determined by the MRCI + Q/V5Z calculations, with the aid of module VIBROT in the MOLCAS 7.4 program package,[19] we determine the

vibrational states of each electronic state through solving the nuclear Schrödinger equation when $J = 0$. For each vibrational state of each electronic state, we compute the $G(\upsilon)$ and B_υ for each non-rotating isotopologue. For the $G(\upsilon)$ and B_υ results, although the electronic states $X^1\Sigma^+$ and $A^1\Pi$ have a few experimental results available, the calculated results fit very well to them, and as for other states $^1\Delta$, $^1\Sigma^-$, $^3\Sigma^+$, $^3\Pi$, $^3\Delta$, $^3\Sigma^-$, $^5\Sigma^+$, $^5\Pi$, and $^1\Pi$ (III) (except for four repulsive states $^5\Delta$, $^5\Sigma^+$ (II),$^1\Pi$ (II), and $^1\Pi$ (IV)), we could not find any experimental data on the AsO^+ radical in the literature. In order to compare with future laboratory experiments or theoretical calculation, we collect the presently available $G(\upsilon)$ and B_υ values of the eleven electronic states for AsO^+ radical in Table 3. In view of excellent agreement of the spectroscopic and molecular properties between the present results and the experimental data shown in Table 2, we believe that the results in Table 3 should be reliable and accurate. Owing to the length of this article, here, we tabulate the values of $G(\upsilon)$ and B_υ of the first 10 vibrational states only for the eleven electronic states, respectively.

Table 3. Values of vibrational energy level $G(\upsilon)$, inertial rotation constant B_υ of the electronic states.

$X^1\Sigma^+$						
	$G(\upsilon)/cm^{-1}$		B_υ/cm^{-1}			
	This work	Exp.[a]	This work	Exp.[b]	Exp.[c]	Exp.[d]
0	547.73	549.1	0.511399	0.4900	0.52050	0.51840
1	1634.95	1642.1	0.508165	0.4845	0.51531	0.438604
2	2711.55	2737.6	0.504955			
3	3777.71	3795.6	0.501712			
4	4833.73		0.498441			
5	5879.73		0.495151			
6	6915.65		0.491870			
7	7941.25		0.488607			
8	8956.33		0.485367			
9	9960.76		0.482142			
$A^1\Pi$						
	$G(\upsilon)/cm^{-1}$		B_υ/cm^{-1}			
	This work	Exp.[a]	This work	Exp.[b]	Exp.[c]	Exp.[d]
0	394.24	388.5	0.443528			
1	1173.53	1154.4	0.439520	0.4148	0.44025	0.4420
2	1939.15	1905.5	0.435302	0.4090	0.44250	0.4376
3	2689.97	2641.6	0.430915	0.4048		0.4278
4	3425.39	3362.9	0.426351			
5	4144.37	4069.2	0.421556			
6	4845.62	4760.7	0.416468			
7	5527.58	5437.4	0.411032			
8	6188.60	6099.0	0.405205			
9	6826.81		0.398860			
	$^1\Delta$		$^1\Sigma^-$		$^3\Sigma^+$	
	This work		This work		This work	
	$G(\upsilon)/cm^{-1}$	B_υ/cm^{-1}	$G(\upsilon)/cm^{-1}$	B_υ/cm^{-1}	$G(\upsilon)/cm^{-1}$	B_υ/cm^{-1}
0	348.59	0.398229	355.96	0.398678	369.60	0.404563
1	1056.70	0.395982	1061.40	0.395534	1102.72	0.401511
2	1762.48	0.392184	1757.89	0.392320	1827.83	0.398442
3	2443.96	0.388264	2445.26	0.389089	2544.10	0.395331
4	3115.81	0.385131	3123.68	0.385863	3251.77	0.392245
5	3778.89	0.381658	3793.19	0.382620	3951.03	0.389141
6	4430.76	0.378085	4453.72	0.379348	4641.59	0.385993
7	5071.81	0.374552	5105.10	0.376033	5323.21	0.382815
8	5703.18	0.371250	5747.13	0.372684	5995.90	0.379638
9	6327.28	0.368245	6379.80	0.369316	6659.99	0.376522
	$^3\Pi$		$^3\Delta$		$^3\Sigma^-$	
	This work		This work		This work	
	$G(\upsilon)/cm^{-1}$	B_υ/cm^{-1}	$G(\upsilon)/cm^{-1}$	B_υ/cm^{-1}	$G(\upsilon)/cm^{-1}$	B_υ / cm^{-1}
0	422.05	0.458384	369.56	c0.403678	359.69	0.399776
1	1257.72	0.454655	1102.57	0.400693	1072.57	0.396655
2	2082.32	0.450906	1827.40	0.397682	1777.33	0.393597
3	2895.58	0.447090	2543.73	0.394660	2474.00	0.390511
4	3697.34	0.443248	3251.97	0.391670	3162.08	0.387372
5	4487.61	0.439380	3952.28	0.388663	3841.48	0.384226
6	5266.14	0.435462	4644.38	0.385615	4512.21	0.381054
7	6032.58	0.431474	5328.04	0.382541	5174.09	0.377858
8	6786.61	0.427408	6003.24	0.379460	5827.29	0.374708
9	7527.90	0.423259	6670.13	0.376408	6472.51	0.371643

Table 3. (*Continued*).

	$^5\Sigma^+$		$^5\Pi$		$^1\Pi$ (III)	
	This work		This work		This work	
	$G(\upsilon)$/cm^{-1}	B_υ/cm^{-1}	$G(\upsilon)$/cm^{-1}	B_υ/cm^{-1}	$G(\upsilon)$/cm^{-1}	B_υ/cm^{-1}
0	158.67	0.245645	83.51	0.238280	259.18	0.297754
1	471.09	0.242657	241.99	0.230805	772.87	0.297215
2	776.94	0.239630	390.34	0.223411	1277.63	0.296461
3	1076.25	0.236558	528.52	0.215197	1773.64	0.295566
4	1368.89	0.233447	656.35	0.206809	2260.28	0.294408
5	1654.83	0.230289	774.25	0.198219	2737.16	0.293034
6	1933.98	0.227083	881.60	0.188642	3204.08	0.291429
7	2206.30	0.223830	977.86	0.178408	3660.64	0.289575
8	2471.72	0.220518	1062.87	0.167316	4106.32	0.287453
9	2730.15	0.217151	1135.83	0.154668	4540.45	0.285035

[a]Data from Ref. [7]; [b]Data from Ref. [10]; [c]Data from Ref. [12]; [d]Data from Ref. [13].

3.3. Potential energy curves of 6Ω electronic states

Once the spin–orbit coupling effect is introduced into the computation, the Λ–S electronic states $X^1\Sigma^+$, $A^1\Pi$, and $^3\Pi$ split into six Ω electronic states, namely, 0^+, 0^-, 0^+, 1, 1, and 2, which hold different dissociation limits $As^+(^3P_0)+O(^3P_2)$ and $As^+(^3P_1)+O(^3P_2)$. And the energy interval is 1047.51 cm^{-1} between the two dissociations, which is in good agreement with the corresponding observed value 1063.49 cm^{-1}.[25] The calculated states with their dissociation limits are listed in Table 4. Based on the calculated PECs, the spectroscopic constants of six Ω electronic states are determined.

Figure 2 shows the calculated PECs of six Ω states and Table 5 lists the spectroscopic constants of the bound states $X^1\Sigma^+_{0+}$, $^3\Pi_{0-}$, $^3\Pi_{0+}$, $^3\Pi_1$, $^3\Pi_2$, and $A^1\Pi_1$. Once the spin–orbit coupling effect is introduced into the computation, the energy interval between two different dissociation limits are rather large, it can be found obviously in Fig. 2. For ground state $X^1\Sigma^+_{0+}$, it consists of the Λ–S state $X^1\Sigma^+$ (100%) and is uninfluenced by the SOC effect in the bound area, so the spectroscopic parameters R_e, D_e, T_e, ω_e, $\omega_e x_e$, and B_e are almost the same as those of the ground state $X^1\Sigma^+$ from the calculation of the Λ–S state. Compared with the calculated results, the calculated dissociation energy D_e of 6.72 eV is 0.03 eV lower than the corresponding value without considering the SOC effect.

Table 4. Dissociation-limit relationships of the 6Ω electronic states.

Atomic state ($As^+ + O$)	Ω state	Energy/cm^{-1}	
$^3P_0+^3P_2$	0^+	0	0
$^3P_1+^3P_2$	0^-, 0^+, 1, 1, 2	1047.51	1063.49[a]

[a]Data from Ref. [25].

Table 5. Spectroscopic constants of the 6Ω electronic states.

Ω state	T_e/cm^{-1}	R_e/nm	ω_e/cm^{-1}	$\omega_e x_e$/cm^{-1}	B_e/cm^{-1}	D_e/eV	Dominant Λ–S states
$X^1\Sigma^+_{0+}$	0	0.15789	1095.02	5.067	0.512972	6.84	$X^1\Sigma^+$ (100%)
Theory[a]	0	0.1568	1100.7	4.83	0.5199	–	
Theory[b]	0	0.15770	1091.07	5.02	0.5148	–	
Exp.[c]	0	0.1568	1091.32	5.00	0.5199	–	
$^3\Pi_{0-}$	35558.18	0.16667	851.01	5.512	0.46039	2.2545	$^3\Pi$ (99.99%)
$^3\Pi_{0+}$	35580.57	0.16667	849.20	5.209	0.46040	2.2518	$^3\Pi$ (99.99%)
$^3\Pi_1$	36087.34	0.16667	849.96	5.916	0.46039	2.1693	$^3\Pi$ (99.98%)
$^3\Pi_2$	36720.52	0.16665	847.69	5.129	0.46051	2.1061	$^3\Pi$ (99.99%)
$A^1\Pi_1$	42306.81	0.16943	779.62	7.336	0.44549	1.4170	$A^1\Pi$ (100%)
Theory[a]	42599	0.1687	780.77	7.36	0.4491	–	
Theory[b]	42327.96	0.16982	776.84	6.72	0.4433	–	
Exp.[c]	42594.2	0.1688	780.8	7.4	0.4491	–	

[a]Data from Ref. [7]; [b]Data from Ref. [8]; [c]Data from Ref. [14].

As shown in Fig. 2, the energies of the four components of the $^3\Pi$ state are superposed in a range of $r < 0.13$ nm, and their energy splittings increase in the the sequence of 0^-, 0^+, 1, and 2, in a range of 0.13 nm $< r <$ 0.28 nm. The excitation energy interval from $^3\Pi_{0-}$ to $^3\Pi_{0+}$ is as small as 22.4 cm^{-1}, while the obvious separations of the $^3\Pi_{0+}$–$^3\Pi_1$ and $^3\Pi_1$–

$^3\Pi_2$ states are 506.77 cm^{-1} and 633.18 cm^{-1} respectively. Comparing the Λ–S electronic state $^3\Pi$ that we have calculated with $^3\Pi_{0-}$, $^3\Pi_{0+}$, $^3\Pi_1$, and $^3\Pi_2$ about the spectroscopic constants, we can obtain that the gaps are −413.63 cm^{-1}, −391.24 cm^{-1}, 115.53 cm^{-1}, and 748.71 cm^{-1} on T_e; 49.88 cm^{-1}, 48.07 cm^{-1}, 48.83 cm^{-1}, and 46.56 cm^{-1} on ω_e; 0.0922 eV, 0.0894 eV, 0.0069 eV, and −0.0564 eV on D_e. Then, we can find that the spectroscopic constants of $^3\Pi$ state are considerably influenced once the spin–orbit couplings effect is taken into account. Especially for the T_e, the values of $^3\Pi_{0-}$ and $^3\Pi_{0+}$ are significantly reduced, but the $^3\Pi_1$ and $^3\Pi_2$ are obviously increased. It shows that the spin–orbit couplings effect has a great effect on the Λ–S electronic state $^3\Pi$.

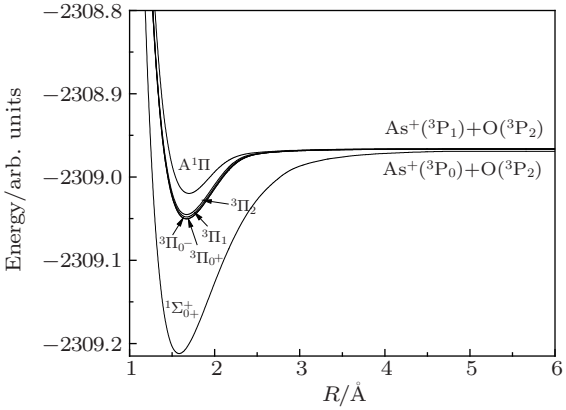


Fig. 2. Potential energy curves of the 6Ω electronic states.

As for the Ω electronic state $A^1\Pi_1$, it completely comes from the Λ–S electronic state $A^1\Pi$. Under the SOC effect, the dissociation energy D_e has a little increase. Moreover, there is a little influence on the excitation energy T_e. It decreases from 42558.88 cm^{-1} to 42306.81 cm^{-1}. But all in all there is little difference between the calculated values and the experimental data,[7,8,14] which is because the $A^1\Pi_1$ state does not have any crossover with other states.

3.4. Transition properties of $A^1\Pi_1$–$X^1\Sigma^+_{0+}$ and $^3\Pi_1$–$X^1\Sigma^+_{0+}$

Figure 3 shows the computed transition dipole moments from $A^1\Pi_1$, $^3\Pi_1$ states to the ground state $X^1\Sigma^+_{0+}$ of the AsO^+ radical, each as a function of the inter-nuclear distance. The dipole moment of the transition from $A^1\Pi_1$ state to the ground-state is much greater than those of the other transitions. At the same time, the TDM of $A^1\Pi_1$ state is reduced strongly with the increase of bond length. Further analysis may show that the former belongs to the singlet–singlet allowed transition, while the latter to the triplet–singlet forbidden transition. The above analysis result can explain why the TDM of the former is much larger than that of the latter.

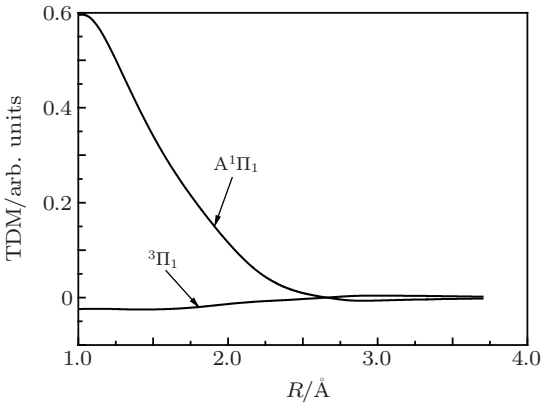


Fig. 3. The TDMs for the transitions from $A^1\Pi_1$, $^3\Pi_1$ states to the ground state $X^1\Sigma^+_{0+}$.

4. Conclusions

The PECs of 15 Λ–S states correlated to $As^+(^3P_g)$ + $O(^3P_g)$ and $As^+(^1D_g)$ + $O(^1D_g)$ are calculated based on the MRCI + Q/V5Z method, in which the states $^1\Delta$, $^1\Sigma^-$, $^3\Sigma^+$, $^3\Pi$, $^3\Delta$, $^3\Sigma^-$, $^5\Sigma^+$, $^5\Pi$, $^5\Delta$, $^5\Sigma^+$ (II), $^1\Pi$ (II), $^1\Pi$ (III), and $^1\Pi$ (IV) are reported for the first time and they could provide an instructive guide for further studying the spectroscopic property. The corresponding spectroscopic constants, vibrational levels, and inertial rotation constants of bound states are determined and they are very close to the available experimental results. The spin–orbit coupling effect calculations are also for the first time used for the studying the AsO^+ radical. When the spin–orbit coupling effect is considered, there is a little influence on spectroscopic constants and dissociation limits of the AsO^+ radical, especially for the $^3\Pi$ state. It splits into four Ω states and the corresponding energy arrangement from low to high is in the sequence of 0^-, 0^+, 1, 2. The calculated energy interval of 0^-–0^+ is only 22.4 cm^{-1}, while the energy intervals of 0^+–1 and 1–2 states are 506.77 cm^{-1} and 633.18 cm^{-1} respectively. The TDMs of $A^1\Pi$–$X^1\Sigma^+_{0+}$ and $^3\Pi_1$–$X^1\Sigma^+_{0+}$ are evaluated, which shows that the former is singlet–singlet allowed transition, while the latter is triplet–singlet forbidden transition. The analysis of the main electron configurations shows that electronic states are multi-configurational in nature, especially for $^1\Pi$ (III) state, and it is essential to employ a multi-configuration method in the accurate and reliable electronic structure calculation.

References

[1] Shi D H, Liu Y F, Sun J F and Zhu Z L 2006 *Chin. Phys.* **15** 1015
[2] Liu Y F, Sun J F, Ma H and Zhu Z L 2007 *Chin. Phys.* **16** 680
[3] Shi D H, Sun J F, Zhu Z L and Liu Y F 2007 *Chin. Phys.* **16** 2701
[4] Zhang X N, Shi D H, Zhu Z L and Sun J F 2010 *Chin. Phys. B* **19** 053401
[5] Liu Y F and Jia Y 2011 *Chin. Phys. B* **20** 033106
[6] Yu B H, Dai Q R, Shi D H and Liu Y F 2007 *Chin. Phys.* **16** 2962

[7] Lakshman S V J and Rao T V R 1971 *J. Phys. B: At. Mol. Opt. Phys.* **4** 269
[8] Wang J M, Shi D H and Zhu Z L 2012 *Acta Phys. Sin.* **61** 153105 (in Chinese)
[9] Lakshman S V J and Rao P T 1960 *Indian J. Phys.* **34** 278
[10] Santaram C V V S N K and Rao P T 1962 *Proc. Phys. Soc.* **79** 1093
[11] Rao D V K and P T Rao 1970 *J. Mol. Phys.* **3** 430
[12] Lakshman S V J 1966 *Proc. Phys. Soc.* **89** 774
[13] Shanker R, Singh I S and Singh O N 1969 *Can. J. Phys.* **47** 1601
[14] Rao D V K and Rao P T 1969 *Curr. Sci.* **38** 384
[15] Huber K P and Herzberg G 1979 *Constants of Diatomic Molecules* Vol. 4 (New York: Van Nostrand Reinhold) p. 46
[16] Langhoff S R and Davidson E R 1974 *Int. J. Quantum Chem.* **8** 61
[17] Richartz A, Buenker R J and Peyerimhoff S D 1978 *J. Chem. Phys.* **28** 305
[18] Werner H J and Knowles P J, MOLPRO, a Package of *ab initio* programs, Version 2008.1, http://www.molpro.net
[19] Krogh J W, Lindh R, Malmqvist P A and Roos B O 2009 MOLCAS 7.4 program package, Lund University
[20] Knowles P J and Werner H J 1985 *Chem. Phys. Lett.* **115** 259
[21] Werner H J and Knowles P J 1988 *J. Chem. Phys. Lett.* **89** 5803
[22] Knowles P J and Werner H J 1988 *Chem. Phys. Lett.* **145** 514
[23] Werner H J and Knowles P J 1985 *J. Chem. Phys.* **82** 5053
[24] Knowles P J and Werner H J 1985 *Chem. Phys. Lett.* **115** 259
[25] Sansonetti J E, Martin W C and Young S L 2005 *Handbook of Basic Atomic Spectroscopic Data* (Phys. Chem. Ref. Data) **34** 1594